Available online at www.sciencedirect.com
SCIENCE DIRECT
Journal of Electrostatics 64 (2006) 450–455
Journal of ELECTROSTATICS
www.elsevier.com/locate/elstat

Filamentary actuation on the surface of bodies contoured by high-speed flows

M. Cabaleiro, G. DiPrimio, G. Artana*

Department of Mechanical Engineering, University of Buenos Aires, Paseo Colon 850, Ciudad de Buenos Aires 1063, Argentina

Available online 14 November 2005

Abstract

In this study, we focus our attention on the ability of a filamentary discharge to affect the shock waves patterns generated by a test model of diamond shape placed in a high-speed airflow. Our results indicate that no significant changes could be detected at moderate supersonic regimes (Ma$\approx$1.8) or at transonic conditions (Ma$\approx$0.8) even when the filament traversed the shock.

Keywords: Electroaerodynamics; Flow control

1. Introduction

In recent years there has been a growing interest in using weakly ionized gases (plasmas) in high-speed aerodynamics. The electrohydrodynamic (EHD) technologies have been considered as good candidates to reduce the wave and viscous drag, heat fluxes, or to produce sonic boom mitigation and boundary layer or turbulent transition control [1]. Shock wave control has application in different areas including supersonic and hypersonic vehicles, gas turbines, reaction motors and so forth.

An electric discharge in a gas flow results in a different amount of gas heating depending on the characteristics of the plasma. This heating, as well as other non-thermal effects from the plasma, such as the "ionic wind", or more complex ones as ion acoustic waves, electron heat conduction, double layer (charge separation), streamer/shock interactions, etc. can affect the flow and can be used for high-speed flow control [2,3].

The actuation on the flow based on these effects is in any case largely dependent on the discharge regime considered. In the past, different configurations with corona discharges [4–6], dielectric barrier discharges [7] or devices enabling to produce volumetric plasmas have been tested [8]. Some research works with devices that produce arcs or sparks have also been undertaken [9].

Filamentary discharges have also been investigated in supersonic and hypersonic flow regimes. These discharges can be very non-uniform both spatially and temporally, and can be created by different strategies like using high-frequency discharges or microwave discharges.

From a technological point of view, a system with a DC or low-frequency discharge has a simpler arrangement, and can be more easily implemented in different applications. With these kinds of excitations, the filamentary actuation may be achieved when the flow velocities attain important values, as the discharge regimes may destabilize and have a tendency towards filamentation [10,11].

For devices based on the filamentary discharge different discharge–airflow interactions have been proposed based mainly on the local alteration of the physical properties of the gas produced by the thermal effect.

Some authors suggested [12] that the filaments traversing a shock wave could serve as a mechanism to equalize the pressure on both sides of the discontinuity. The filament would act in this case as some porous devices that are usually mounted on the surface of blades or airfoils to alter the shock wave patterns.

Other works [3] proposed to couple the thermal gradients induced by the discharge with bow shock waves to produce vortices at the interfaces between the hot and

*Corresponding author. Fax: +54 11 43 31 18 52.
E-mail address: gartana@fi.uba.ar (G. Artana).

0304-3886/$ - see front matter
doi:10.1016/j.elstat.2005.10.028

cold zones. The vorticity generation being a dissipative process should lead to a dissipation of the shock's energy.

More recently, Samimy et al. [13] proposed that the localized increase in pressure produced by the gas heating would act in a similar manner to a solid obstacle such as a tab suddenly placed in the flow. Repetitive pulsing of the discharge would enable control over the "obstacles", and if the frequency could be suitably tuned excitation of preferred instabilities modes could be achieved.

The gas temperature inside the filaments [12,14,15] is directly related to the amount of energy deposition. So, the electric power is a critical parameter that affects the performance of the devices, but it has to be considered with others variables as filament size, location and free stream Mach number [16]. The effects achieved on the flow are also quite sensitive to the region where the discharge acts. When actuation occurs in inviscid gas flow regions (volume plasma actuation) it requires much more energy than when it acts in the viscid flow regions close to the surface of the body (surface plasma actuation) [17]. Recent results indicate that with suitable electrode arrangements the surface devices require only moderate power peaks (≈ 30 W) or currents peaks (≈ 0.2 A) in contraposition to conventional volume plasma devices that use current peaks of several amperes and short duration.

A requirement of devices with reduced current peaks is of interest not only from an efficiency point of view but also to reduce some associated problems as electrode or surface erosion and also to reduce electromagnetic radiation.

In this work, we analyze a flow configuration given by an aerodynamic optimized model placed in a high-speed flow. The objective is to analyze the ability of a filamentary discharge to alter the pattern of attached shock waves when the discharge traverses the discontinuity region. The actuation considered occupies a region close to the surface of the model produced by filaments disposed in the direction of the flow.

2. Experimental set-up

2.1. Wind tunnel

An induction supersonic wind tunnel with a test section of 101.6 mm × 25.4 mm has been used in our experiments. Its Laval nozzle was composed by fixed pieces and exchangeable pieces of different geometries that enabled to achieve different Mach numbers (maximum Ma = 1.8). A set of 25 holes enabled the measurement of the pressure in ports disposed at different stream-wise stations of the nozzle.

The model was held by inserts that enter the holes of the visualization windows and enabled the positioning of the model in the test section. These windows could rotate to orient the model at the desired angle. The conditions of pressure and temperature at the entrance of the Laval nozzle were fixed by room conditions.

2.2. Models

The models tested were diamond-shaped (semi angle 6°) bodies. They were constructed of PMMA with surface flush-mounted electrodes made of aluminium foils (Fig. 1). The interelectrode spacing was 7.4 mm. Two small holes on the upper and lower surface enabled to determine the surface pressure of the diamond model. The wire connection and tubing exited the test section through the mountings.

2.3. Schlieren system

A Schlieren system has been used to visualize the density field gradients of the compressible flow. It was composed of concave mirrors (diameter = 101.6 mm, focal lengths = 1.3 and 0.9 m), a quasi-point light source, a single border knife-edge and a digital video camera, disposed in a *z* arrangement.

2.4. Pressure measurement system

Pressure measurements on the surface of the models (upper and lower surface) and on the Laval nozzles have been undertaken connecting the ports by electrical insulating tubing to absolute and differential piezoresistive sensors (measurement ranges of 0–100 and 0–50 kPa).

2.5. Electric measurement system

The electrodes were attached to HV DC sources (0 ± 30 kV–30 W) as indicated in Fig. 4. Current measurements were made with an optoisolator circuit (accuracy of 1 μA passband filtering 0–1 kHz). The device is quite similar to the one described in a previous report [18] and converts the current signal to a voltage signal. This signal is then amplified and recorded through a data acquisition system (Fig. 2).

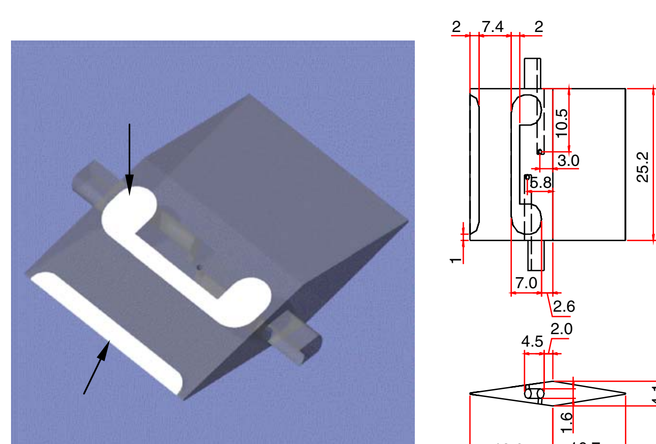

Fig. 1. Diamond-shaped model (sizes in mm). Arrows show the electrodes.

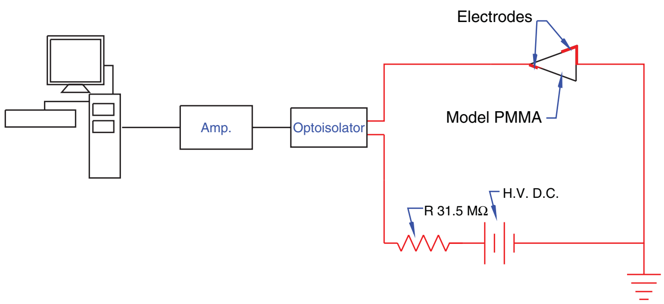

Fig. 2. Schematic of the current measurement system.

3. Experimental results

The models were tested at different air stream velocities and considering different configurations (Fig. 1):

- Position 1 refers to the situation when the electrode is located at the leading edge meanwhile,
- Position 2 denotes the situation when the model is rotated 180° and the electrode is at the trailing edge and faces downstream regions,
- Polarity 1 refers to upstream electrode at HV and the downstream one earthed and
- Polarity 2 is the opposite situation of Polarity 1.

All the tests were carried out with an angle of attack of 0°. The steady state was achieved for a maximum of 25 s, depending on the Laval nozzle considered.

3.1. Discharge regimes

The experimental procedure consisted on fixing the electrode potentials and then establishing the air flow. The discharge observed without airflow and prior to the opening of the valve was a diffuse discharge (Fig. 3a).

When the steady conditions of the flow were established different discharge regimes could be observed and we identified two filamentary regimes: fixed filaments and multiple moving filaments (Figs. 3b and c). In the fixed regime one or two filaments occupied always the same position during the test and occurred when the stressed electrode was at the leading or trailing edge of the model. In the multiple moving the number of filaments increased and occupied different positions during the test and occurred when the grounded electrode was at the leading or trailing edge. The discharge regimes so established were arc free and enabled an operation without damage of the HV sources. The diffuse discharge could turn to an impulsive arc discharge when the flow was imposed if the voltage difference established exceeded an upper value. This upper limit was a function of the flow condition considered.

A typical current vs time curve of the experiment may be observed in Fig. 4. In this graph the airflow starts at about 5 s, is followed by the steady flow regime (from about 7 to 17 s) and from about 17–32 s the vessel is emptied but not at constant velocity. Current peaks associated to the surface filamentary discharge may be observed in these graphs all along the test period. They are of reduced

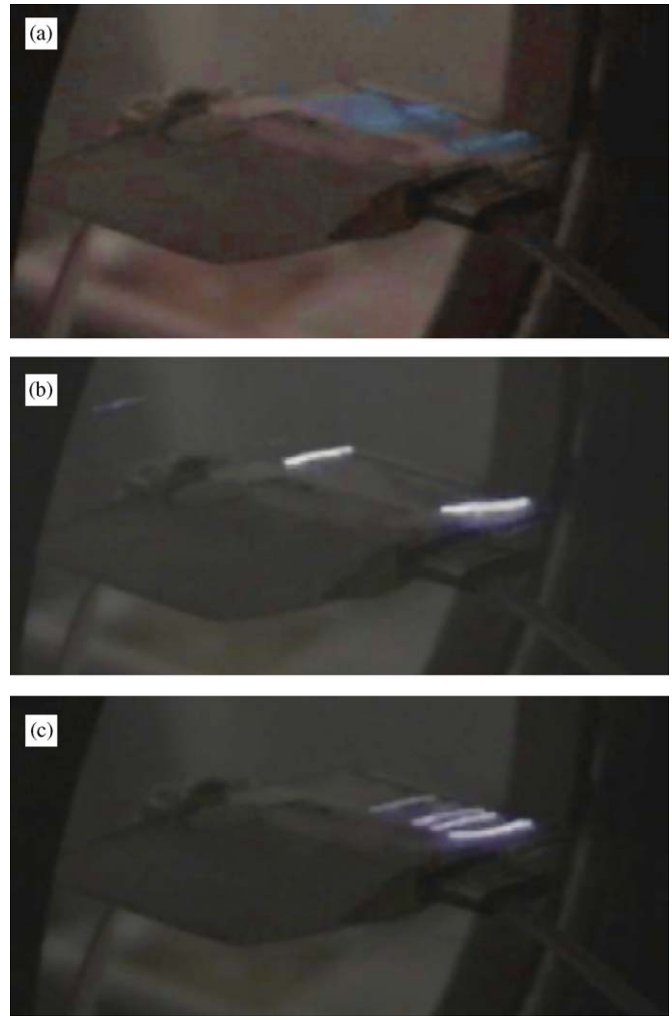

Fig. 3. (a): Diffuse discharge in conditions without airflow. (b) Fixed filamentary discharge; Polarity 1 (upstream electrode at HV)—Position 1; free air stream Ma = 1.8. (c) Moving filamentary discharge; Polarity 2 (downstream electrode at HV)—Position 1; free air stream Ma = 1.8.

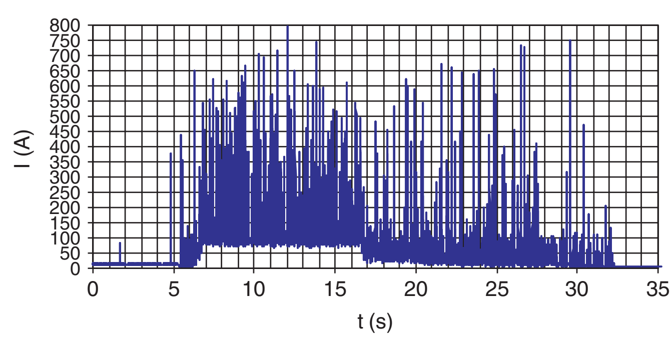

Fig. 4. Current vs. time, moving Filamentary discharge regime: Position 2/Polarity 1 (upstream electrode at HV), $V = 6.5\,kV$. Free air stream Ma = 1.8.

intensity (<1 mA) but as a consequence of the long duration of the test the time resolution of the acquisition is not enough to observe the real peak magnitudes that are very short in time. All the peaks during the steady regime develop from an almost constant threshold value (in Fig 4 close to 0.08 mA). This threshold depends on the flow characteristics and on the electrode arrangement.

Voltage-current curves that characterize the different tests can be constructed considering the threshold values or the time averaged values of the steady regimes as both values are directly related. We represent these curves for the different cases in Figs. 5 with maximum values of the voltage difference fixed considering arc free situations.

An analysis of these figures reveals that higher the velocities, higher the currents (time-averaged or threshold values). However, higher the velocities, higher the difficulties to achieve stable (arc free) discharges.

Also, we can observe that Polarity 1 configuration (upstream electrode at HV) enables one to achieve higher values of currents compared to the Polarity 2 configuration (downstream electrode at HV), and that the moving filamentary regime (Position 1/Polarity 2 or Position 2/Polarity 1) gives higher values than the fixed filamentary regime (Position 1/Polarity 1 or Polarity 2/Position 2).

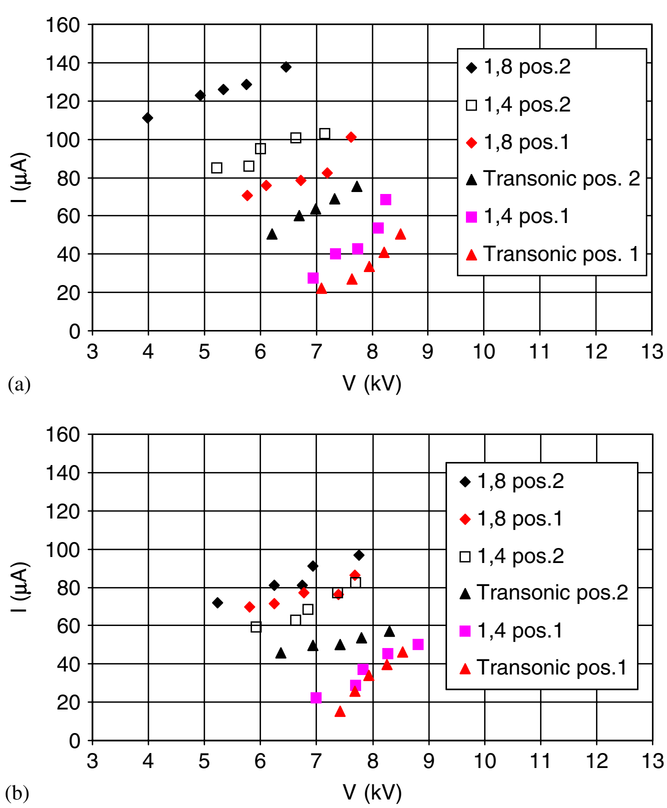

Fig. 5. (a) Current (time averaged values) vs. applied voltage Polarity 1 (upstream electrode at HV), different Laval nozzles (Ma $\approx$ 1.8, 1.4 and transonic); (b) current (time averaged values) vs. applied voltage Polarity 2 (downstream electrode at HV), different Laval nozzles (Ma $\approx$ 1.8, 1.4 and transonic).

3.2. Flow measurements

In this section, we show some typical results of actuations when filaments traverse the shock wave when the electrode is disposed in the leading edge (Fig. 6a) or in the trailing edge (Fig. 6b).

In both cases the analysis of the pressure on the ports upstream of the model enables to determine that the flow attacks the models with a Mach number (Ma_1) close to 0.9. The free air stream accelerates around the model and passes to a supersonic regime. In the interelectrode space, lambda-type shock waves were observed. These shock waves were traversed by the filaments of the discharge.

The Schlieren photos or surface pressure measurements for the case with discharge on, in moving or fixed filamentary regimes, showed no significant global differences compared to no discharge (not shown).

It is quite probable that the discharge could have produced some local changes of the shock wave patterns. However, we could not observe any evidence of it, and on the Schlieren images splitting or alterations of the thickness of the shock waves could not be detected.

We have undertaken other tests (not shown in this paper) with the same model but at other Mach number ($Ma_1 \approx 1.4$ and 1.8) with other shock wave patterns (not traversed by the filament), and with a dihedral-shaped model (semi angle of 4.5° and a length of 20 mm, flow conditions: $Ma_1 \approx 0.8$, 1.4 and 1.8) with similar electrode arrangements and filamentary regimes. They have also shown negligible effects on the shock wave [19].

4. Conclusion

We have analyzed discharge regimes characterized by the presence of filaments disposed at close vicinity of the surface of the model. We propose the following conclusions of our work:

- When electrodes are flush-mounted on the surface of the body and voltage differences are imposed with DC HV, fixed filaments or moving filaments regimes may be observed.
- The first regime occurs when the electrode connected to positive HV is at the leading or trailing edge.
- The currents passing through the filaments increase as the free air stream velocity increases (or the pressure decreases) and the moving filament regime enables higher currents.
- The filamentary discharges were parallel to the flow and did not affect either the pressure on surface of the test model or the shock wave patterns for a given Mach number even when they traversed the discontinuity created by the shock.

Further research efforts should be undertaken considering discharge regimes with a larger number of filaments of higher current or stable discharges, covering more

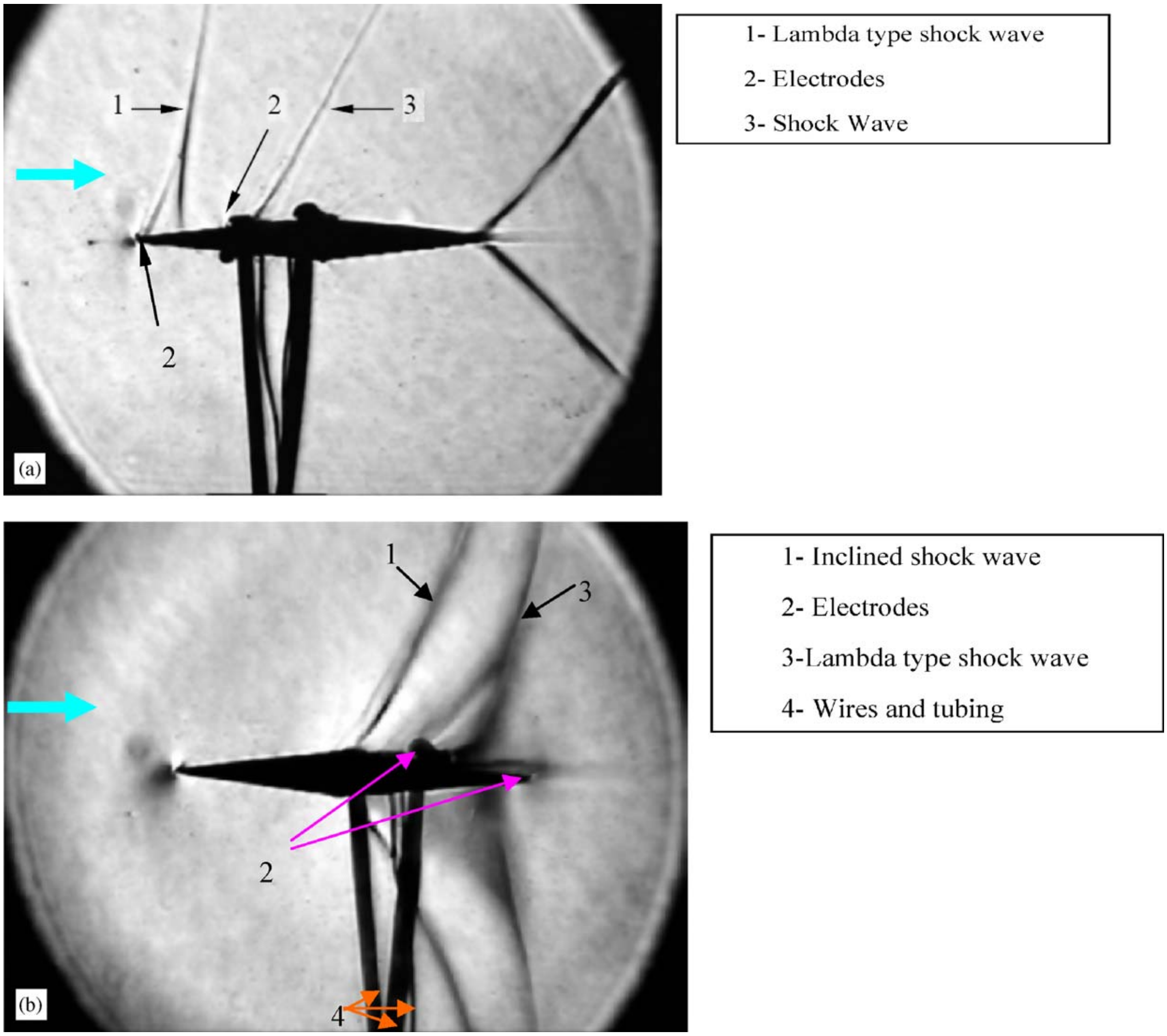

Fig. 6. (a) $Ma_1 = 0.92$, Position 1 (the flow is subsonic and accelerates around the model to supersonic); (b) $Ma_1 = 0.88$, Position 2 (the flow is subsonic and accelerates around the model to supersonic).

uniformly the interelectrode space, to conclude on the ability of the plasma surface actuation to control the shock waves on aerodynamically optimized devices.

Acknowledgments

This research has been done with Grants UBACYT I024 and PICT 12-09482 of the Argentine government.

References

[1] V. Semenov, V. Bondarenko, Gildenburg, V. Gubchenko, A. Smirnov, Weakly ionized plasmas in aerospace applications, Plasma Phys. Control. Fusion 44 (2002) B293–B305.
[2] E. Daso, W. Beaulieu, J. Hager, Prediction of drag reduction in supersonic and hypersonic flows with counterflow jets, AIAA paper 2002-5115, 2002.
[3] P. Bletzinger, B. Ganguly, D. Van Wie, A. Garscadden, Plasmas in high speed aerodynamics, J. Phys. D Appl. Phys. 38 (2005) R33–R57.
[4] M.S. Cahn, G.M. Andrew, Electroaerodynamics flow, AIAA Paper No. 68-24, 1968.
[5] S. Cheng, A. Goldburg, An analysis of the possibility of sonic boom by electro-aerodynamic devices, AIAA Paper No. 69-38, 1969.
[6] A. Klimov, S. Leonov, A. Pashina, V. Skvortov, T. Cain, B. Timofeev, Influence of a corona discharge on the supersonic drag of an axisymmetric body, AIAA paper 99-4856, 1999.
[7] T. Corke, D. Cavalieri, E. Matlis, Boundary-layer instability on sharp cone at Mach 3.5 with controlled input, AIAA J. 40 (5) (2001) 1015–1018.
[8] S. Merriman, E. Ploenjes, P. Palm, I. Adamovich, Shockwave control by nonequilibrium plasmas in cold supersonic gas flows, AIAA Paper 2000-2327, 2000.
[9] M. Minucci, R. Bracken, L. Myrabo, H. Nagamatsu, K. Shanahan, Experimental investigation of an electric arc simulated air spike in hypersonic flow, AIAA paper 2000-0715, 2000.
[10] S. Kuo, D. Bivolaru, Electric discharges in the presence of supersonic shocks, Phys. Lett. A 313 (2003) 101–105.
[11] Yu.P. Raizer, Gas Discharge Physics, Springer, Berlin, 1991.
[12] S. Leonov, V. Bityurin, A. Klimov, Y. Kolesnichenko, Influence of structural electric discharges on parameters of streamlined bodies in airflow, AIAA paper 2001-3057, 2001.
[13] M. Samimy, I. Adamovich, B. Webb, J. Kastner, J. Hileman, S. Keshav, P. Palm, Development and characterization of plasma actuators for high speed jet control, Exp. Fluid. 37 (2004) 577–588.

[14] S.C. Leonov, V. Bityurin, Y. Kolesnichenko, Dynamic of a single-electrode HF filament in supersonic airflow, AIAA Paper 2001-0493, 2001.

[15] V. Soloviev, V. Krivstov, A. Konchakov., N. Malmuth, Drag reduction by plasma filaments over supersonic forebodies, AIAA J. 41 (12) (2003) 2403–2409.

[16] J. Wilkerson, D. van Wie, B. CybyK, Numerical assessment of heterogeneous plasma discharge effects on supersonic forebody drag, AIAA Paper 2003-0526, 2003.

[17] S. Macheret, M. Shneider, R. Miles, Magnetohydrodynamic and electrohydrodynamic control of hypersonic flows of weakly ionized plasmas, AIAA Paper 2002-2249, 2002.

[18] J.C. Fothergill, J.A. Houlgreave, A simple optical method for measuring currents at high voltages with an example of use on a coronating electrode in air, IEE Conference on Dielectric Materials, Measurements and Applications, 24–27 September 1996, Bath.

[19] J.M. Cabaleiro, Control de Flujos compresibles con actuadores EHD, Tesis de Ingenieria, FIUBA, 2004, http://www.fi.uba.ar/laboratorios/lfd.